

NUMERICAL SIMULATION OF SOLIDS FLOW IN A BLAST FURNACE

S. J. ZHANG¹, A. B. YU¹, P. ZULLI², B. WRIGHT² and P. AUSTIN²

¹School of Materials Science and Engineering, University of New South Wales, Sydney, NSW 2052, Australia

²BHP Steel Research Laboratories, P. O. Box 202, Port Kembla, NSW 2505, Australia

ABSTRACT

This paper presents a numerical study of the behavior of solids flow in a two-dimensional blast furnace. The investigation considers the layer-charging of materials (iron-bearing and coke) and solids consumption (e.g. coke combustion in the raceway) and is based on a previously developed solids flow model (Zhang et al., 1998). Input data includes the ore and coke profiles, productivity, and solids volume loss due to shrinkage, meltdown, reduction and combustion as determined from typical operating conditions. The results demonstrate that the mass loss strongly affects the solids flow pattern and deadman profile in a blast furnace.

Keywords: solids flow, blast furnace, solid consumption, numerical simulation

NOMENCLATURE

d_p	particle diameter, m
g	gravity, m/s^2
p	pressure, Pa
S	solid consumption rate, $kg/m^3 \cdot s$
u	velocity vector, m/s
β	gas-particle momentum transfer coefficient, $kg/m^3 \cdot s$
ϵ_s^*	volume fraction of solid particles (-)
ϵ	volume fraction (-)
ϕ_i	internal friction angle ($^\circ$)
ϕ_s	sphericity of particle (-)
ϕ_w	wall friction angle ($^\circ$)
μ	viscosity, $kg/m \cdot s$
ρ	density, kg/m^3
τ	stress tensor (-)

Subscripts

g	gas
s	solid

INTRODUCTION

Numerical modeling of flow in granular (or solids) systems remains an active area for research due to the difficulties in adequately describing the physics associated with particle-particle and fluid-particle interactions. In broad terms, two numerical approaches are applied to modeling solids flow *viz.* discrete element and continuum.

In the discrete element approach, the motion of individual particles is considered with no need for global assumptions such as steady-state behavior, uniform constituency, and/or constitutive relations. Though this approach has been applied to the simulation of solids flow in 2D and 3D hoppers (Langston et al., 1995), its disadvantage is in computational efficiency, particularly in investigations of more practical problems.

In the continuum approach, the principles of continuum mechanics are utilized i.e. solids or fluid mechanics. Investigations based on solid mechanics provide satisfactory predictions for the stress field but not so for the velocity field (Jenike et al., 1968, 1973; Walker, 1966; Nguyen et al., 1979; Haussler et al., 1984; Runesson et al., 1986). Models based on fluid mechanic principles include plug flow, potential flow, kinematic (Listwinski, 1963; Mullins, 1972 and 1974) and viscous flow (Chen et al., 1993). All are limited to an extent: in the case of both plug and potential flow, the formulations are too simplistic to simulate solids flow satisfactorily; the kinematic model can predict solids flow for systems with simple geometry, e.g. central hopper flow (Nedderman and Tuzun, 1978) but is unable to predict the velocity discontinuity and stagnant zones commonly observed in such systems (Nedderman, 1995); the viscous flow model (Chen et al., 1993) requires knowledge of the stagnant zone profile *a priori* and this may be difficult to obtain for a system with a complicated geometry.

To overcome the aforementioned limitations, a model describing the solids flow under blast furnace conditions with gas flow has been developed by Zhang et al. (1998). In this model, the surface stress resulting from the interaction amongst flowing particles is considered to be composed of two parts: rate-dependent and rate-independent. Moreover, a method is developed to determine the transition between moving and stationary zones.

In a blast furnace (BF), iron-bearing (ore, sinter and/or pellets) and coke materials are charged alternatively in batches, resulting in a layered packing, or burden, structure. These materials then undergo physical and chemical changes as they descend within the furnace, including shrinkage, meltdown, reduction and combustion ("solids consumption"); furthermore, the extent of each reaction is dependant on its location within the furnace (Omori, 1987). The layered packing structure and solids consumption in the furnace may significantly affect the solids flow, as reported by Takahashi et al. (1996).

The purpose of the paper is to extend the numerical model reported by Zhang et al. (1998) to investigate the effects of layered burden and solids consumption on solid flow in a BF.

THEORETICAL TREATMENTS

Governing Equations

In an Eulerian frame of reference, the governing equations for the flow of solid particles can be generally written as:

$$\frac{\partial \varepsilon_s}{\partial t} + \nabla \cdot (\varepsilon_s \mathbf{u}_s) = 0 \quad (1)$$

and

$$\frac{\partial (\rho_s \varepsilon_s \mathbf{u}_s)}{\partial t} + \nabla \cdot (\rho_s \varepsilon_s \mathbf{u}_s \mathbf{u}_s) = \nabla \cdot \boldsymbol{\tau}_s + \rho_s \varepsilon_s \mathbf{g} \quad (2)$$

Since particles may flow in a manner similar to a fluid, or be stagnant like a solid and provide a resistance to the moving particles, their surface stress, $\boldsymbol{\tau}_s$, may be considered to consist of two parts (Johnson et al., 1987 and 1990; Hutter et al., 1994)

$$\boldsymbol{\tau}_s = \boldsymbol{\tau}_{rd} + \boldsymbol{\tau}_n \quad (3)$$

where $\boldsymbol{\tau}_{rd}$ is rate-dependent and stems from the particle-particle kinetic interaction due to collision, while $\boldsymbol{\tau}_n$ is rate-independent and stems from the particle-particle contact interaction due to packing, including normal contact and shear friction. In general, $\boldsymbol{\tau}_s$ depends on ε_s , $\nabla \varepsilon_s$ and D_s , in which ε_s is the volume fraction of particles, and D_s the stretching tensor associated with the motion of particles. In this work, $\boldsymbol{\tau}_{rd}$ and $\boldsymbol{\tau}_n$ are determined by using the conventional Newtonian expression and Coulomb frictional stress model, respectively (Hutter et al., 1994; Savage, 1983; Norem et al., 1987).

The consumption of solids in the lower part of the BF takes into account shrinkage (reduction) and meltdown of ore, and gasification, carbonization and combustion of coke. With these considerations, the continuity and momentum equations for a two-dimensional, steady-state, gas-solid flow system are expressed as:

a) For solid phase

$$\nabla \cdot (\varepsilon_s \mathbf{u}_s) = S \quad (4)$$

and

$$\nabla \cdot (\rho_s \varepsilon_s \mathbf{u}_s \mathbf{u}_s) = -\varepsilon_s \nabla p - \beta (\mathbf{u}_s - \mathbf{u}_g) + \nabla \cdot \boldsymbol{\tau}_{rd} + \nabla \cdot \boldsymbol{\tau}_n + S \mathbf{u}_s + \rho_s \varepsilon_s \mathbf{g} \quad (5)$$

b) For gas phase

$$\nabla \cdot (\varepsilon_g \mathbf{u}_g) = 0 \quad (6)$$

and

$$\nabla \cdot (\rho_g \varepsilon_g \mathbf{u}_g \mathbf{u}_g) = -\varepsilon_g \nabla p - \beta (\mathbf{u}_g - \mathbf{u}_s) + \nabla \cdot \boldsymbol{\tau}_g + \rho_g \varepsilon_g \mathbf{g} \quad (7)$$

where

$$\varepsilon_g + \varepsilon_s = 1 \quad (8)$$

The flow of gas under BF conditions is turbulent and is described by a standard k- ε turbulence model. The two-dimensional blast furnace model used in the physical and mathematical modeling is shown in Fig. 1. Details regarding the constitutive equations, the evaluation of physical parameters, the turbulence model, the calculation

of momentum transfer coefficient β and the boundary conditions may be found elsewhere (Zhang et al., 1998).

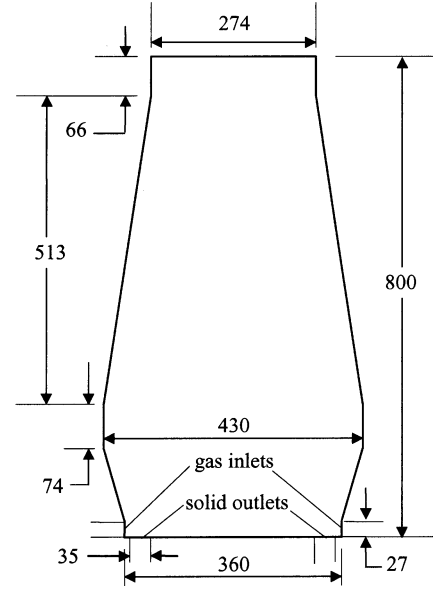


Figure 1: Blast furnace model geometry (unit: mm)

Determination of the Stagnant Zone

Generally, there are two distinct zones in a solid flow field: stagnant and flow zones. For BF operational control, it is very important to identify the boundary between the two zones. There has been some success in predicting the velocity distribution in the active flow region, but as yet there are no simple and satisfactory methods for the determination of the stagnant-active flow zone transition. At present, there are two alternate methods for predicting the velocity distribution and the profile of stagnant zone: (1) based on the plasticity theory (Nedderman, 1992), the stagnant and flow zones are determined utilizing static and dynamic mechanics, respectively; and (2) once the velocity field is determined, the stagnant zone is prescribed by defining the stagnant zone boundary as that beyond which the particles move with a velocity less than a specified or critical value (Tuzun et al., 1982). As discussed earlier, the general application of (1) is difficult, particularly for flow systems with complicated geometry. Takahashi et al. (1989) proposed a simplified approach to overcome this difficulty but it cannot be used generally.

In the present work, the stagnant region is determined using an approach following Tuzun et al (1982). It is noted that the critical solid velocity is usually determined by experimentation; the present work suggests that this critical solid velocity is $1/9d_p$ per minute. In the determination of the velocity field, the stagnant region is effectively motionless and its profile should be treated as a boundary, which implies an important modification of the approach of Tuzun et al. (1982). Hence, the computational domain for the solid (and gas) phase varies, such that a new stagnant zone profile is generated for each iteration. However, it can be shown that the so obtained stagnant zone converges, giving a numerically stable profile as, for example, shown in Fig. 2(a). Moreover, a few iterations can lead to a converged stagnant zone profile (Fig. 2(b)).

The solution procedure employed in this study is given below:

1. Determine the initial solid velocity field under the boundary conditions at the inlet, outlet and walls of the container;
2. Determine the stagnant region and calculate its area;
3. Re-calculate the solid velocity field, with the profile of the stagnant zone profile as part of the boundaries (note that particle-particle friction is used for this boundary);
4. Determine a new stagnant region, and compare its area with the previous one (the difference is used as a residual); and
5. Repeat steps 3 and 4 until convergence (when the residual is below a preset value).

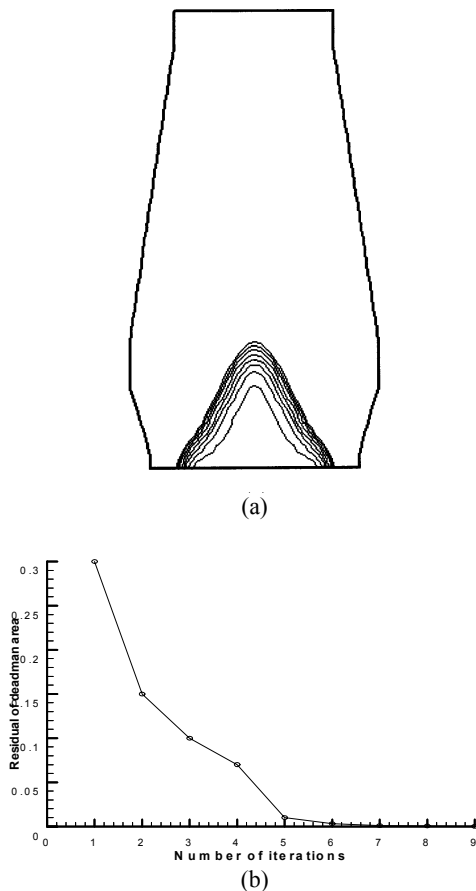


Figure 2. Typical example of computation showing the convergence of the stagnant zone profile (Glass beads, solid flowrate=200 g/min, no gas flow).

Numerical Method

The two sets of conservation equations, closed with the constitutive equations and supplemented with the initial and boundary conditions, cannot be solved analytically and therefore a numerical technique must be used to obtain an approximate solution. Stewart and Wendroff (1984) have reviewed the techniques with respect to the numerical modeling of multiphase flow systems. The numerical method used in the present study is based on a finite volume method developed by Spalding (1983), which is essentially the application of the SIMPLE method to multi-phase flow. The inter-phase slip algorithm (IPSA) is used to treat all terms in the governing

equations implicitly; hence, time step limitations usually encountered in explicit finite differencing techniques, are removed. The calculation domain is represented by a number of fixed Eulerian cells through which the gas-solid dispersion moves. A non-staggered grid is utilized, complimented with the Rhie-Chow method (1983) to eliminate the odd-even decoupling of pressure. The scalar variables (void fraction and pressure) and velocity components are all defined at the cell centers. The partial derivative in time is replaced by a simple first-order approximation. For the discretization of the convective transport terms in the two sets of conservation equations, the deferred correction technique, suggested by Khosla and Rubin (1974), has been used, which is implicit upwind plus explicit central finite difference. For the discretization of viscous transport terms in the momentum equations, the central finite difference approximation with second-order spatial truncation errors has been used.

RESULTS AND DISCUSSION

Validation of the Present Model

To test the assumptions made in the present model, a comparison between model predictions and measurements made using a scaled-down blast furnace model was carried out. The model geometry and layout are shown in Fig. 1. Glass beads (GB) and plastic beads (PB) are used as bulk materials (see Table 1). Other experimental details can be found elsewhere (Wright et al., 1996).

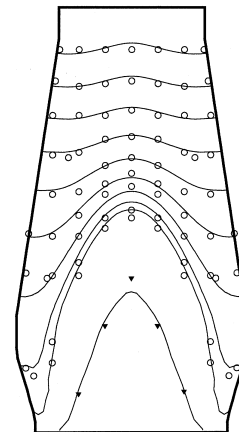


Figure 3: Time lines (o, measured; —, calculated) and stagnant zone (v, measured; - - -, calculated) profile when GB flowrate = 200 g/min, air flowrate = 28.8 m³/h.

Fig. 3 shows the measured time lines (3 minute intervals) together with the computed results. It is evident that good agreements exists; furthermore, the solids flow domain can be described via three regions: (1) plug flow in the upper part of the furnace; (2) a stagnant zone in the central part of the furnace; and (3) an active flow channel, through which most particles descend smoothly into the discharge ports. After passing below the “transition” from the upper to the lower parts, solid particles move towards the discharge ports through the converging flow channel bounded by the stagnant zone and the side wall. The active flow channel can be recognized as being in a state of core flow. Adjacent to the stagnant zone, the flow of solid particles is very slow, giving a so-called quasi-stagnant zone (Takahashi et al., 1989; Wright et al, 1996). The existence

of the quasi-stagnant zone can also be confirmed from long tail in the resident time distribution as shown in Fig. 4.

Table 1: Physical properties of glass beads, plastic beads and their mixture

	d_p (m)	ρ_s (kg/m ³)	ϵ_s^*	ϕ_w (°)	ϕ_i (°)	ϕ_s
GB	0.003	2500	0.58	20	26	1
PB	0.00275	1400	0.43	20	34	0.6
Mix.*	0.00283	1641	0.47	20	30.8	0.86

* Mixtures = $0.33 \times \text{GB} + 0.67 \times \text{PB}$ (vol. fraction)

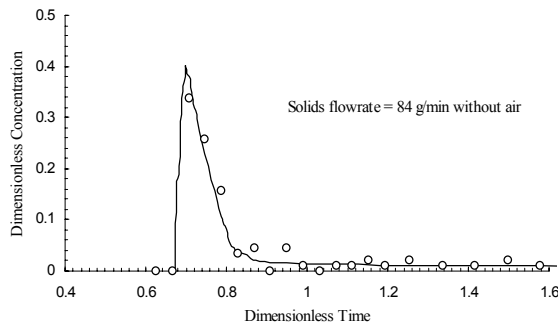


Figure 4: Comparison between measured (o) and predicted (-) residence time distributions.

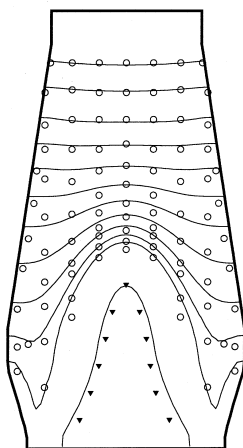


Figure 5: Time lines (o, measured; —, calculated) and stagnant zone profile (∇, measured; - - -, calculated) for the flow of a mixture of glass/plastic beads (solids flowrate = 58 kg/min, without air flow).

In practice, ore and coke are charged into a blast furnace layer by layer. However, the assumption of packing homogeneity is required to effect a numerical simulation and obtain a high computational efficiency. Recently, Wright et al. (1996) confirmed via experimentation that this assumption is acceptable. To demonstrate the applicability of the present model to solids flow in the blast furnace, simulations have also been performed for a mixture of glass and plastic beads. In this computation, the physical properties required were simply taken as the harmonic mean based on the solid volume fractions (also listed in Table 1). As shown in Fig. 5, the computed time lines are in good agreement with those measured, suggesting that the present treatments can provide

satisfactory predictions of solids flow patterns in a blast furnace.

Simulations with Layered Burden and Mass Loss

With layered ore and coke in blast furnace modeled as a homogeneous mixture, the numerical simulation of solids flow in a blast furnace can be simplified significantly. Conversely, in practice, it is useful to trace the flow of individual ore and coke layers. This information can be used to predict the thickness of the fused ore layer and coke slit in the cohesive zone, which is directly linked to the re-distribution of gas in the zone. Using mass balances, the structure of ore and coke layers can be calculated as an outcome of the present model, particularly when the porosity of either ore or coke is assumed to be constant. For the purpose of comparison, unless specified, all cases considered below are under the conditions same as those for Fig. 5.

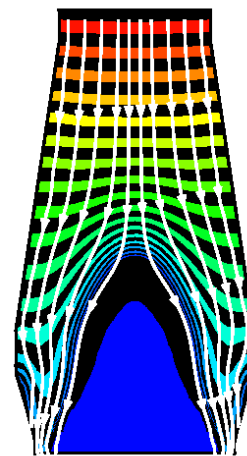


Figure 6: Layered flow pattern with uniform initial burden.

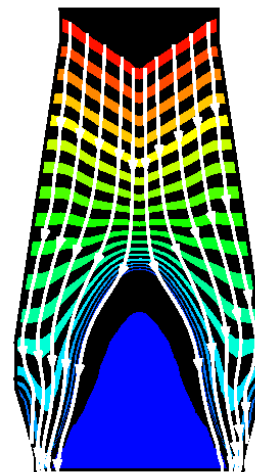


Figure 7: Layered flow pattern with “V-shaped” initial burden.

Figs. 6 and 7 illustrate the computed layered flow structure under two alternate initial burden distributions: uniform and “V-shaped”. The initial distributions of ore and coke at the top of the burden can be obtained from an empirical model or measurement or the combination of the two. The results in Figs. 6 and 7 suggest that the change of

initial burden distribution affects the inner distribution of ore and coke but does not change the profile of stagnant zone or deadman because of the homogeneous assumption.

During its downward flow, iron ore is heated while reacting with the upward flowing gas; in particular, within a certain temperature range, the ore softens and melts, generating liquid iron and slag which flow into the furnace hearth. On the other hand, coke flows toward the raceway where it is consumed by reaction with oxygen in the blast; to a much less extent, coke is also consumed in other zones of the furnace, e.g. solution loss and the carbon transfer to liquid metal in the dripping zone, deadman and the furnace hearth. Therefore, the solid consumption rate S ($\text{kg}/\text{m}^3\cdot\text{s}$) varies in a blast furnace. In this work, it is determined as follows:

- (1) Above the cohesive zone, the consumption is negligible, so that

$$S = 0$$
- (2) In the cohesive zone, iron ore will be fully consumed as a result of softening and melting, i.e.

$$S = (S_{\text{flowrate}} \times \text{OSM}) / (\text{CCO} \times \text{VOL}_{\text{cz}})$$
- (3) Below the cohesive zone, the coke consumption is given as

$$S = (S_{\text{flowrate}} \times \text{CSO}) / (\text{CCO} \times \text{VOL}_{\text{bcz}})$$
 to represent the coke solution loss, and

$$S = (S_{\text{flowrate}} \times \text{CTM}) / (\text{CCO} \times \text{VOL}_{\text{bot}})$$
 to represent the carbon transfer to the metal in the hearth in addition to the coke combustion in the raceway.

Here, OSM is the ore shrinkage and meltdown in the cohesive zone, CCO the coke combustion at the raceway, CSO the coke solution in the dripping zone and deadman, and CTM the coke transfer to metal in the hearth. S_{flowrate} is the solid flowrate at outlet equivalent to the coke combustion at the raceway. Once the location of the cohesive zone is known, its volume VOL_{cz} , the volume below the cohesive zone VOL_{bcz} and the volume of the furnace hearth VOL_{bot} can be determined.

To examine the effect of solid consumption or mass loss on solids flow, the present numerical simulation is carried out using typical operational data. That is, the values of CCO, CSO, CTM and OSM are 370, 90, 40 and 1660 kg per ton of hot iron, respectively. The computer code is so developed that it can account for a different shape and location of the cohesive zone. However, for convenience, only inverse V-shaped cohesive zone is considered in this paper, noting that in practice.

Figs. 8 and 9 show the flow patterns of solids as they undergo layered burden and solids consumption, for the same initial burden distributions used in Figs. 6 and 7. The solids consumption has a very strong effect on the behavior of solids flow, with the deadman becoming much smaller, the flow patterns indicate the walls have stronger effects. When ore and coke flow under gravity with mass loss, the velocities of solid particles within the furnace are necessarily increased in order to maintain the same solid flowrate S_{flowrate} . As a result, the active particles impact more strongly those that are stagnant (and without mass loss), reducing the size of stagnant zone and which, in turn affects the solids flow pattern in the furnace.



Figure 8: Layered flow pattern with solids consumption and uniform initial burden.



Figure 9: Layered flow pattern with solids consumption and non-uniform initial burden.

Fig. 10 shows the effect of overall mass loss rate on solid flow patterns. The conditions are the same as those used to generate the results in Fig. 9 but with the coke (solids) consumption rate in BF varied. Hence, the coke and ore charge rates at the top are affected. The results suggest that for a given cohesive zone, as the productivity increases, the solids velocity will increase and the size of stagnant zone decreases.

CONCLUSIONS

The solids flow model of Zhang et al. (1998) has been extended to study the solids flow with layered burden and solids consumption in a blast furnace. The results demonstrate that the solids consumption has a very strong effect on the flow pattern and the stagnant zone. In general, increasing the solids consumption rate will increase the solids velocity and decrease the size of stagnant zone.



Figure 10. Flow patterns when the overall mass loss rate is: (a) double; and (b) half of that in Fig. 9.

ACKNOWLEDGEMENTS

The authors would like to thank Australian Research Council and BHP for financial support.

REFERENCES

- CHEN, J. Z., AKIYAMA, T., NOGAMI, H., YAGI, J. I. and TAKAHASHI, H., (1993), "Modeling of solid flow in moving beds," *ISIJ Int.*, 33(6), 664-671.
- HAUSSLER, U. and EIBL, J., (1984), "Numerical investigation on discharging silos," *J. Eng. Mech., ASCE*, 110 (6), 957-971.
- HUTTER, K. and RAJAGOPAL K. R., (1994), "On flows of granular materials," *Continuum Mech. Thermodynamics*, 6, 81-139.
- JENIKE A. W. and JOHANSON, J. R., (1968), "Bin loads," *J. Struct. Div., ASCE*, 94(4), 1011-1041.
- JENIKE, A. W., JOHANSON, J. R. and CARSON, J. W., (1973), "Bin loads-part 2: concepts," *J. Eng. for Industry, ASME*, 95, 1-16.
- JOHNSON, P. C. and JACKSON, R., (1987), "Frictional-collisional constitutive relations for granular materials, with application to plane shearing," *J. Fluid Mechanics*, 176, 67-93.
- JOHNSON, P. C., NOTT, P. and JACKSON, R., (1990), "Frictional-collisional equations of motion for particulate flows and their application to chutes," *J. Fluid Mechanics*, 210, 501-535.
- KHOSLA, P. K. and RUBIN, S. G., (1974), "A diagonally dominant second-order accurate implicit scheme," *Computers and Fluids*, 2, 207-209.
- LANGSTON, P. A., TUZUN, U. and HEYES, D. M., (1995), "Discrete element simulation of granular flow in 2D and 3D hoppers: dependence of discharge rate and wall stress on particle interactions," *Chem. Eng. Sci.*, 50(6), 967-987.
- LISTWINISZYN, J., (1963), "The model of a random walk of particles adapted to researches on problems of materials of loose materials," *Bull. l'Academie Polonaise Sci.*, 11, 61-70.
- MULLINS, W., (1972), "Stochastic theory of particle flow under gravity," *J. Appl. Phys.*, 43(2), 665-678.
- MULLINS, W., (1974), "Nonsteady-state particle flow under gravity-an extension of the stochastic theory," *J. Appl. Mech., ASME*, 44, 867-872.
- NEDDERMAN, R. M., (1992), "Statics and kinematics of granular materials", Cambridge University Press.
- NEDDERMAN, R. M., (1995), "The use of the kinematic model to predict the development of the stagnant zone boundary in the batch discharge of a bunker," *Chem. Eng. Sci.*, 50(6), 959-965.
- NEDDERMAN, R. M. and TUZUN, U., (1978), "A kinematic model for the flow of granular materials," *Powder Technol.*, 22, 243-253.
- NGUYEN, T., BRENNEN, C. and SABERSKY, R. H., (1979), "Gravity flow of granular materials in conical hoppers," *J. Appl. Mech. ASME*, 79-WA/APM-20.
- NOREM, H., IRGENS, F. and SCHIELDROP, B. A., (1987), "A continuum model for calculating snow avalanches". In: *Avalanche formation, movement and effects*, ed. By Salm, B. and Gubler, H., IAHS Publ., 126, 363.
- OMORI, Y., (1987), "Blast furnace phenomena and modeling," Elsevier Applied Science, London.
- RHIE, C. M. and CHOW, W. L., (1983), "A numerical study of the turbulent flow past an isolated airfoil with trailing edge separation," *AIAA Journal*, 21, 1525-1532.
- RUNESSON, R. and NISSON, L., (1986), "Finite element modeling of the gravitational flow of a granular material," *Bulk Solids Handling*, 6(5), 877-884.
- SAVAGE, S. B., (1983), "Granular flows down rough inclines-review and extension". In: *Mechanics of granular materials: new models and constitutive relations*, ed. by JENKINS, J. T and SATAKE, M., Elsevier, 261.
- SPALDING, D. B., (1983), "Developments in the IPSA procedure for numerical computation of multiphase-flow phenomena with interphase slip, unequal temperature, etc." In: Shih, T. M., ed., *Proc. 2nd Nat. Symp., "Numerical properties and methodologies in heat transfer"*, Hemisphere, New York, 421-436.
- STEWART, H. B. and WENDROFF, B., (1984), "Two-phase flow: models and methods", *J. Comp. Phys.*, 56, 363-409.
- TAKAHASHI, H., KUSHIMA, K. and TAKEUCHI, T., (1989), "Two dimensional analysis of burden flow in blast furnace based on plasticity theory," *ISIJ Int.*, 29(2), 117-124.
- TAKAHASHI, H., TANNO, M. and KATAYAMA, J., (1996), "Burden descending behavior with renewal of deadman in a two dimensional cold model of blast furnace," *ISIJ Int.*, 36(11), 1354-1359.
- TUZUN, U., HOULSBY, G. T., NEDDERMAN R. M. and Savage, S. B., (1982), "The flow of granular materials," *Chem. Eng. Sci.*, 37(12), 1691-1709.
- WALKER, D. M., (1966), "An approximate theory for pressures and arching in hoppers," *Chem. Eng. Sci.*, 21(8), 975-997.
- WRIGHT, B., ZULLI, P. ZHANG, S. J. and YU, A. B., (1996), "Study of Flow behavior of granular material with model blast furnace under normal and abnormal conditions," Internal Research Report, BHP Research.
- ZHANG, S. J., YU, A. B., ZULLI, P., WRIGHT, B. and TUZUN, U., (1998), "Modeling of the solids flow in a blast furnace," *ISIJ Int.*, 38(12), 1311-1319.